Response to Editor's and Referees' Comments on Manuscript hess-2020-91 "A new criterion for determining the representative elementary volume of translucent porous media and inner contaminant" by Ming Wu, Jianfeng Wu, Jichun Wu, and Bill X. Hu

Note that the following text in Arial Narrow font denotes Editor's and Reviewers' comments and in Times New Roman font denotes our response to the comments in the review. In our Supplement (pdf/zip), the PDF file has clearly indicated all changes to the original manuscript. In our Manuscript (pdf), all changes have been included in the clean version of the revised PDF file. Also, in our marked PDF file, marked in a green strikethrough font is the text that should be removed from the original manuscript and marked in a red font is the text that has been added to the revision. In addition, Line number(s) mentioned below is referred to as that line numbering in the marked revised manuscript.

Response to Anonymous Referees' Comments

We received two review reports submitted by two anonymous referees. Report #1 from Referee #3 suggested the manuscript should be "accepted as is"; Report #2 submitted by Referee #1 suggested the manuscript should be "accepted subject to minor revisions". Suggestions for revision are as follows:

(1) Line 44, references are suggested to add before "Previous studies... ".

[Response] References are added after "Previous studies" (Line 44).

(2) Line 590, Table 2 represents the parameter, not equations! Title should be revised.

[Response] We have revised the title of Table 2 as the referee suggested (Lines 592-593).

A new criterion for determining the representative elementary volume of

translucent porous media and inner contaminant

Ming Wu[1, 2], Jianfeng Wu[2*], Jichun Wu[2], and Bill X. Hu[1*]

[1] Institute of Groundwater and Earth Sciences, Jinan University, Guangzhou 510632,

China

[2] Key Laboratory of Surficial Geochemistry, Ministry of Education; Department of

Hydrosciences, School of Earth Sciences and Engineering, Nanjing University, Nanjing

210023, China

Correspondence to: J.F. Wu (jfwu@nju.edu.cn), B.X. Hu (billhu@jnu.edu.cn)

12   **ABSTRACT**

13   Representative elementary volume (REV) is essential to measure and quantify the effective

14   parameters of a complex heterogeneous medium. To overcome the limitations of the existing

15   REV estimation criteria, a new REV estimation criterion (χ^i) based on dimensionless range

16   and gradient calculation is proposed in this study to estimate REV of a translucent material

17   based on light transmission techniques. Three sandbox experiments are performed to

18   estimate REVs of porosity, density, tortuosity and perchloroethylene (PCE) plume using

19   multiple REV estimation criteria. In comparison with χ^i, previous REV estimation criteria

20   based on the coefficient of variation (C_V^i), the entropy dimension (DI^i) and the relative

21   gradient error (ε_g^i) are tested in REV quantification of translucent silica and inner PCE

22   plume to achieve their corresponding effects. Results suggest that new criterion (χ^i) can

23   effectively identify the REV in the materials, whereas the coefficient of variation   and

24   entropy dimension (DI^i) are not effective. The relative gradient error   can make the

25   REV plateau obvious, while random fluctuations make the REV plateau uneasy to

26   identify accurately. Therefore, the new criterion is appropriate for REV estimation of the

27   translucent materials and inner contaminant. Models are built based on Gaussian equation

28   to simulate the distribution of REVs for media properties, which frequency of REV is dense

29   in the middle and sparse on both sides. REV estimation of PCE plume indicates high level

30   of porosity lead to large value of mean and standard deviation for REVs of PCE saturation

31   (S_o) and PCE-water interfacial area (A_{OW}). Fitted equations are derived from distribution of

32   REVs for PCE plume related to d_m (distances from mass center to considered point) and d_I

33   (distances from injection position to considered point). Moreover, relationships between

2

REVs of PCE plume and S_o are fitted using regression analysis. Results suggest a decreasing

trend appears for S_o-REV when S_o increases, while A_{ow}-REV increases with increasing of

S_o.

Keywords: new criterion; representative elementary volume (REV); translucent material

1. Introduction

Modelling groundwater and contaminant (such as hazardous irons) transport in

subsurface environment is based on the premise that micro-structure of aquifer exist a

representative elementary volume (REV) (Wang et al., 2016; Lei and Shi, 2019). REV acts

as a micro-scale characteristic, which is important to improve our understanding of

materials, inner fluid flow and other processes (Brown and Hsieh, 2000; Costanza-Robinson

et al., 2011; Wu et al., 2017). Previous studies (Bai et al., 2016; Esfandiar et al., 2017)

suggested that even the Platinum-Nanoparticle-Catalyzed hydrogenation reactions and ion

transport through angstrom-scale slits in cell activity existed apparent size effect, implying

size effect is a wide characteristic for many process and materials (Bai et al., 2016; Esfandiar

et al., 2017). With the help of REV, a porous medium can be treated as continuum medium

(Brown and Hsieh, 2000; Kang et al., 2003; Müller and Siegesmund, 2010; Teruel and

Rizwan-uddin, 2010; Hendrick et al., 2012; Wang et al., 2012; Ukrainczyk and Koenders,

2014; Kim and Mohanty, 2016; Gilevska et al., 2019). A conceptual representation of "REV

curve" (Brown and Hsieh, 2000), characterizing porosity (θ) change with measured scale

(L) increment, is presented in Fig. 1a. Based on the characteristic of REV curve in Fig. 1a,

the REV curve can be divided into three regions. When measured scale (Fig. 1b) is in region

I, the porosity fluctuates drastically at small scales. As measured scale size ranging between

56   L_{min} and L_{max}, a flat plateau with constant and steady value is encountered and the property

57   is factored into its average value. Material property in spatial scales less than L_{min} is spatially

58   varied portions with small scale, which can be easily influenced by individual pores in

59   micro-structure such as region I (Fig. 1a). Likewise, material property is allowed drift to

60   new values in spatial scale above L_{max} due to additional morphological structures of large

61   field heterogeneity (region III). As a matter of fact, REV scale of region II can be derived

62   between the small and spatially varied property in region I and large field variability in

63   region III. However, the lower and upper boundaries L_{min} and L_{max} of REV plateau is hard

64   to be identified in reality (Brown and Hsieh, 2000; Costanza-Robinson et al., 2011).

65   As technology advanced and progressed, non-destructive and non-invasive techniques

66   of x-ray and gamma ray micro-tomography were utilized for micro-structure characteristic

67   measurement in materials (Ghilardi, 1993; Brown and Hsieh, 2000; Niemet and Selker,

68   2001; Bob et al., 2008; Al-Raoush and Papadopoulos, 2010; Costanza-Robinson et al., 2011;

69   Al-Raoush, 2012; Borges and Pires, 2012; Fernandes et al., 2012; Rozenbaum and Roscoat,

70   2014; Pereira Nunes et al., 2016; Piccoli et al., 2019). Generally, REV estimation for

71   material properties, inner gas and fluid also was usually implemented by micro visualization

72   and scanning of X-ray and gramma ray in laboratory (Brown and Hsieh, 2000; Razavi et al.,

73   2007; Nordahl and Ringrose, 2008; Al-Raoush and Papadopoulos, 2010; Costanza-

74   Robinson et al., 2011; Rozenbaum and Roscoat, 2014; Borges et al., 2018), while different

75   criteria were utilized to quantify REV (Brown and Hsieh, 2000; Martínez et al., 2007;

76   Nordahl and Ringrose, 2008; Costanza-Robinson et al., 2011). Lower boundary scale L_{min}

77   of REV was identified by means of entropy dimension (DI^{i}) for eight soil samples (Martínez

4

78 et al., 2007). Further, REV scale of permeability for ripple laminated sandstone intercalated

79 with mudstone was estimated using the coefficient of variation (C_V^i), which the REV scale

80 is identified by the variability among the ten samples to achieve average REV scale

81 (Nordahl and Ringrose, 2008). As a result, only one REV boundary was identified and

82 not every sample can be estimated effectively (Nordahl and Ringrose, 2008). More

83 interestingly, REV of material property (porosity), moisture saturation and air-water

84 interfacial areas in porous media were estimated by a criterion named the relative gradient

85 error (ε_g^i)(Costanza-Robinson et al., 2011). REVs of permeability of translucent material,

86 PCE saturation and PCE-water interfacial area also can be estimated using the relative

87 gradient error (Wu et al., 2017). In summary, the REV estimation was made by multiple

88 kinds of criteria, while the REV identification effects of these criteria were not clear.

89 What's more, these previous criteria estimate REV scale unsatisfactorily that beginning

90 and ending of REV plateau can't be identified simultaneously for translucent porous media

91 based on light transmission technique. Therefore, new criterion which can identify REV

92 plateau accurately is needed.

93 In this study, a new criterion (χ^i) for REV estimation is proposed to identify the REV

94 scale of the translucent silica and inner contaminant. Three perchloroethylene (PCE)

95 transport experiments are conducted in two dimensional (2D) sandboxes to test the effect of

96 different REV estimation criteria. Translucent silica is selected for associated REV analysis

97 due to its extensive utilization in laboratory experiment of exploring groundwater flow and

98 contaminant migration behavior in micro-structure of a sandy aquifer (Niemet and Selker,

99 2001; Bob et al., 2008; Costanza-Robinson et al., 2011). Moreover, translucent silica is also

100 an important material applied in numerous industries (Bouvry et al., 2016). In laboratory

101 experiments, translucent silica is packed in 2D sandboxes where porosity, density, tortuosity

102 and PCE saturation are derived by light transmission technique (Fig. 1c). Porosity and PCE

103 saturation are selected as the representative variables to explore corresponding REV

104 estimation by different criteria, which is very essential and significant for REV

105 identification. Previous criteria such as the coefficient of variation (C_V^i), entropy

106 dimension (DI^i), the relative gradient error (ε_g^i) and the new criterion-χ^i are tested in REV

107 estimation. Associated effects are analyzed to achieve the best criterion of effective and

108 appropriate quantification of REV.

109 **2. Experiment procedure and method**

110 2.1 Experiment

111   Three sandboxes (Fig. 2a-c) packed by translucent silica medium are prepared in

112 laboratory to test different criteria of REV quantification. PCE is selected as a typical

113 DNAPL contaminant used in experiments. 2D sandbox is composed by three aluminum

114 interior frames and two glass walls, which thickness is 1.6cm. The dimensions of sandboxes

115 used in Experiment-I are 20 (width) ×15 (height), and the dimensions of Experiments-II and

116 III are 60 (width)×45 (height). F40/50 and F20/30 mesh translucent silica sands are used for

117 background material for Experiments-I and II, while heterogeneous translucent silica with

118 low porosity and permeability are packed in sandbox for Experiment-III. To make the

119 translucent silica fully saturated by water in a flow field close to natural groundwater

120 environment (Erning et al., 2012), water flow at flow velocity of 0.5 m/d is set from left to

121 right in laboratory sandbox experiments (Fig. 2a-c). Water is restricted in a sandbox that the

top and bottom layers of the sandbox are packed by F70/80 mesh translucent silica as

capillary barriers. Light source is placed behind the sandbox to make light penetrate through

translucent media and capture emergent light intensity using a thermoelectrically air-cooled

charge-coupled device (CCD) camera (Fig. 1c). Afterward, PCE is injected into sandboxes

from the injection needle at constant rate of 0.5 mL /min for three experiments. Detailed

experimental conditions are listed in Table 1.

2.2 Light transmission technique

By means of light transmission technique (Fig. 1c), DNAPL and water saturation can

be obtained rapidly and in real-time, which greatly help to explore the mechanism of

groundwater flow and contaminant migration in porous media. When light passes through

translucent materials of a given thickness, the emergent light intensity after the absorptive

and interfacial losses can be expressed as (Niemet and Selker, 2001; Bob et al., 2008; Wu

et al., 2017):

$$I_T = CI_0(\prod \tau_b)\exp(-\sum \alpha_a d_a) \tag{1}$$

where a represents phase number; b represent the number of the interface between phase a

and $a+1$; I_0 is the original light intensity; C is a constant of correction for light emission

and light observation; τ_b is the transmittance when light penetrate from phase a to $a+1$;

α_a is the absorption coefficient when light penetrate in phase a; d_a is the length of light

penetration path in phase a.

To derive the porosity, the 2D translucent porous medium should be only saturated

by water. Consequently, the emergent light intensity can be expressed as (Niemet and

Selker, 2001; Bob et al., 2008; Wu et al., 2017):

$$I_s = CI_0 \tau_{s,w}^{2k_o} \exp(-\alpha_s k_s d_s) \tag{2}$$

where $\tau_{s,w}^{2k_0}$ is the transmittance of solid-water interface; α_s is solid particles absorption coefficient; d_s is median diameter of the solid particles; k_o is the number of pores across light penetration path; k_s is the number of solid particles across light penetration path.

If we arbitrarily select an infinitesimal element, its area A_o approaches zero ($A_o \to 0$) from the 2D translucent porous media (Fig. 1d), and suppose the infinitesimal element with thickness L_T containing solid particles and pores that can be regarded as lamellar structure (Fig. 1d), we can obtain the following relationships (Wu et al., 2017):

$$\theta A_o L_T = A_o k_o d_o \tag{3}$$

$$k_s d_s + k_o d_o = L_T \tag{4}$$

where d_o is the median diameter of pores; θ is porosity.

Substituting Eq. (3) and Eq. (4) into Eq. (2), the relationship between emergent light intensity and porosity can be achieved (Wu et al., 2017):

$$lnI_s = \beta + \theta\gamma \tag{5}$$

where $\beta = \ln(\dfrac{CI_s}{e^{\alpha_s d_s L_T}})$ and $\gamma = \ln(\tau_{s,w}^{\frac{2L_T}{d_0}} e^{\alpha_s L_T})$. β and γ can be determined from experimental data, then porosity can be obtained.

The density and tortuosity are derived as (Wu et al., 2018):

$$\rho = \theta\rho_w + (1.0 - \theta)\rho_s \tag{6}$$

$$\tau = 1 + \frac{\pi - 2}{\sqrt{\dfrac{\pi}{1 - \theta}}} \tag{7}$$

where ρ is the density of translucent porous media; ρ_w is the density of water; ρ_s is the density of solid particles; τ is tortuosity.

165　　　The saturation of dense nonaqueous phase liquid (DNAPL) was quantified by light

166　　transmission technique based on light pass through translucent materials (Niemet and Selker,

167　　2001; Bob et al., 2008):

$$S_o = \frac{\ln I_s - \ln I_T}{\ln I_s - \ln I_{oil}} \tag{8}$$

169　　where S_o is the saturation of DNAPL; I_s is the light intensity after light penetration through

170　　translucent porous when all pores are fully saturated by water; I_{oil} is the light intensity

171　　when all pores are fully saturated by DNAPL; I_T is the light intensity after penetration

172　　through translucent materials. After quantification of PCE saturation, PCE-water interfacial

173　　area (A_{OW}) can be obtained based on the method proposed by Wu et al. (2017), where the

174　　unit of A_{OW} is cm^{-1}.

175　　　　Emergent light intensity for three experiments is captured by a thermoelectrically air-

176　　cooled charge-coupled device (CCD) camera (Niemet and Selker, 2001; Bob et al., 2008).

177　　Every pixel with small scale could be approximated as infinitesimal element in high

178　　resolution image to apply light transmission techniques. As consequence, porosity of

179　　translucent silica was derived using light transmission technique through Eq. (5). The whole

180　　2D translucent silica area was numerically discretized that every cell had the uniform

181　　dimensions of 0.015m×0.015m. The cuboid window (Fig. 1b) was utilized to quantify the

182　　variables (porosity, density, tortuosity, PCE saturation, PCE-water interfacial area) of every

183　　cell as measured scale was increased. In detail, the measured cuboid window scale was

184　　increased from the center of each cell and associated value of variable was calculated from

185　　the high resolution porosity of 2D translucent silica derived by light transmission technique.

186　　Observation cells were selected from the discretized cells (Fig. 3b) of which the cells I-1~2,

187 II-1~2 and III-1~2 belong to Experiments-I-III, respectively.

188 To analyze the regularity of REV distribution for PCE plume, the mass center

189 coordinate and the granglia-to-pool ratio (GTP) of PCE plume are quantified for

190 Experiments-I-III. The mass center coordinate and GTP are calculated as:

191
$$X_m = \frac{M_{10}}{M_{00}} \tag{9}$$

192
$$Z_m = \frac{M_{01}}{M_{00}} \tag{10}$$

193
$$GTP = \frac{V_{ganglia}}{V_{pool}} \tag{11}$$

194 where X_m is x coordinate of mass center for PCE plume; Z_m is z coordinate of mass center

195 for PCE plume; GTP is granglia-to-pool ratio, which equals to the ratio of the $V_{ganglia}$ to

196 V_{pool}; $V_{ganglia}$ is the PCE volume under ganglia state; V_{pool} is the PCE volume under pool

197 state; M_{00}, M_{10} and M_{01} are computed using definition of spatial moment (M_{ij}),

198 $M_{ij} = \int_{x_0}^{x_1} \int_{z_0}^{z_1} \theta(x,z) S_o(x,z,t) x^i z^j d_x d_z$; x_0 and z_0 are minimum limits of x axis and z axis; x_1

199 and z_1 are maximum limits of x axis and z axis; $\theta(x,z)$ is the porosity at point (x,z); $S_o(x,z,t)$

200 is PCE saturation of point (x, z) at time t.

201 2.3 Criteria of REV quantification

202 The REV is defined as the volume range in which all material characteristics are

203 factored into the average and associated values approach single and constant (Brown

204 and Hsieh, 2000). In the range of REV, the value of one associated property will meet

205 the condition:

206
$$\frac{\partial Y(L_i)}{\partial L} |_{L_i=L_o} = 0 \tag{12}$$

207 where the $Y(L_i)$ is the value of an associated property when system scale is L_i; L_i is the

208   value of system scale; L_o is the scale range of REV, $L_{min} < L_o < L_{max}$; L_{max} is upper

209   boundary of REV; L_{min} is lower boundary of REV scale. According to the Eq. (12), when

210   the measured scale (L_i) reaches REV range, $\frac{\partial Y(L_i)}{\partial L} \to 0$. As a matter of fact, most

211   previously used criteria were applied to estimate REV based on this requirement (Brown

212   and Hsieh, 2000; Martínez et al., 2007; Nordahl and Ringrose, 2008; Costanza-Robinson

213   et al., 2011).

214   To evaluate the REV of porosity, the coefficient of variation (C_V^i) is utilized to

215   estimate the variability (Nordahl and Ringrose, 2008):

216
$$C_V^i = \frac{\hat{s}_i}{\overline{\varphi}_i} \tag{13}$$

217   where i is the cuboid window (Fig. 1b) increment number; φ is the measured variable,

218   such as porosity; $\hat{s}_i$ is the standard deviation of sub-grids' variable in different measured

219   volume or scale; $\overline{\varphi}_i$ is the arithmetic average of the variable values in the sub-grids.

220   When number of sub-grids (N) is less than 10, a correction is utilized to replace Eq. (13).

221   According to Nordahl and Ringrose (2008), $0 < C_V^i < 0.5$ is defined as homogeneous

222   and $C_V^i = 0.5$ can be used as criterion to identify the REV scale.

223   Similarly, for porosity of translucent silica, entropy dimension (DI^i) is utilized for

224   REV analysis and estimation (Martínez et al., 2007), which is defined as:

225
$$DI^i \approx \frac{\sum_{j=1}^{m(i)} \mu_j(L_\varepsilon) \log \mu_j(L_\varepsilon)}{\log L_\varepsilon} \tag{14}$$

226   where, L_ε is the scale of sub-grid; "$\approx$" indicates the asymptotic equivalence as $L_\varepsilon \to 0$

227   (Martínez et al., 2007); j is the ordinal number of sub-grid in measured cuboid window

228   (Fig. 1b) of increment number i; $m(i)$ is the total number of sub-grids in measured cuboid

229   window (Fig. 1b) of increment number i; $\mu_j(\varepsilon)$ is the proportion of the variable of sub-

grid j in the whole measured cuboid window i. The right hand side of Eq. (14) is the simplification of Shannon entropy of all sub-grids, in which DI^i can be considered as the average of logarithmic values of the variable distribution weighted by $\mu_j(L_\varepsilon)$ to quantify the degree of medium heterogeneity. Using Eq. (14), a series of values of DI^i (i=1,2,3…) are obtained for each measured cuboid window (Fig. 1b) of increment number i. For estimation of the REV in a porous medium, the relative increment of entropy dimension and associated criterion of REV identification are respectively expressed as:

$$RI^i = |\frac{DI^j - DI^{j-1}}{DI^{j-1}}| \times 100 \tag{15}$$

$$RI^i \leqslant 0.2 CV_{DI} \tag{16}$$

where CV_{DI} is the coefficient of variation of DI^i series (i=1,2,3…), which is calculated through $CV_{DI} = (\hat{s}_{DI}/\overline{DI}) \times 100$; $\overline{DI}$ is the mean value of the DI^i series; $\hat{s}_{DI}$ is the standard deviation of the DI^i series.

To achieve the REV for multiple system variables, such as porosity, moisture saturation and air-water interfacial areas in an unsaturated porous medium, a criterion named the relative gradient error was applied (Costanza-Robinson et al., 2011):

$$\varepsilon_g^i = |\frac{\varphi^{i+1} - \varphi^{i-1}}{\varphi^{i+1} + \varphi^{i-1}}| \frac{1}{\Delta L} \tag{17}$$

where ε_g^i is relative gradient error; ΔL is the measured cuboid window size increment length for REV estimation. Usually, ε_g^i less than 0.2 (Costanza-Robinson et al., 2011) is utilized to identify a REV sizes.

According to the requirement in Eq. (12), a new criterion based on the required condition of REV is proposed to estimate the REV range of the translucent silica in this study:

$$\chi^i = \frac{|\delta^{i+1} - \delta^{i-1}|}{\delta^i \Delta L} \tag{18}$$

where δ^i is the dimensionless range, $\delta^i = \frac{\varphi(L_i)_{max} - \varphi(L_i)_{min}}{\overline{\varphi(L_\iota)}}$; $\varphi(L_i)_{max}$ is the

maximum value of the variable on the volume scale L_i; $\varphi(L_i)_{min}$ is the minimum value

of the variable on the volume scale L_i; $\overline{\varphi(L_\iota)}$ is the mean value of the variable on the

volume scale L_i. Brown and Hsieh (2000) suggested $\delta^i = \frac{\varphi(L_i)_{max} - \varphi(L_i)_{min}}{\overline{\varphi(L_\iota)}} << 1$ can

be used for REV estimation. In fact, the calculated value of δ^i mostly is less than 1, while

$\delta^i << 1$ is hard to be used to identify the REV scale for realistic materials, such as the

translucent silica used in this study. The value limit of χ^i used for REV estimation also is

explored in this study.

In this study, criteria for the coefficient of variation (C_V^i), entropy dimension (DI^i),

the relative gradient error (ε_g^i) and the new criterion (χ^i) are all applied to REV estimation

for porosity and PCE saturation. Corresponding REV plateau identification effects are

compared to select the best criterion for REV quantification.

3. Results and discussion

3.1 REV identification effect of different criteria

3.1.1 The coefficient of variation

Emergent light intensity distributions of translucent silica for three experiments, which

had been fully saturated by water, were obtained by a thermoelectrically air-cooled CCD

camera (Niemet and Selker, 2001; Bob et al., 2008). The porosity, density, tortuosity and

PCE saturation for three experiments are derived by light transmission technique as shown

in Figs. 3a and b. The PCE spreads from the injecting point shaped like a drop of water at

t=5 min (Fig. 3b). In 2D sandboxes for three experiments, PCE plume infiltrates in

274   translucent silica sands and reaches the bottom after t=80 min.

275   Porosity and PCE saturation variation curves of all observation cells with increasing

276   measured cuboid window scale were shown in Figs. 4a and b. However, for all observation

277   cells from translucent silica, the REV plateaus were not obvious to be objectively judged

278   visually, which made REV plateaus hard to identify effectively by original variation curves

279   for porosity and PCE saturation (Figs. 4a and b).

280   To make the REV plateau more explicit, different criteria of REV quantification are

281   utilized. The coefficient of variation (C_V^i) of porosity and PCE saturation fluctuating with

282   increasing of measured cuboid window size is shown in Fig. 4. The measured cuboid

283   window scale is limited to the dimensions of cells in discretization of 2D translucent

284   silica. The observation cells show various characteristics of variation tendency for the

285   coefficient of variation (C_V^i). The θ and S_o variation curves of the coefficient of variation

286   (C_V^i) for all observation cells do not reach stable values as those shown in Figs. 4a and b,

287   the beginning of the REV flat plateau is not easy to identify, the coefficient of variation (C_V^i)

288   is not suitable for REV estimation. According to the heterogeneity definition by Corbett and

289   Jensen (1992), the heterogeneity of materials is defined by C_V^i magnitude that $0 <$

290   $C_V^i < 0.5$ is classed as homogeneous medium, $0.5 < C_V^i < 1.0$ is classed as

291   heterogeneous medium and $1.0 < C_V^i$ is classed as strong heterogeneous medium. For

292   the coefficient of variation (C_V^i) magnitude in Figs. 4a and b, the C_V^i values are all below

293   0.5 that the criterion $C_V^i = 0.5$ is unable to identify the REV scale for translucent silica.

3.1.2 Entropy dimension

Entropy dimension (DI^{i}) is utilized by Martínez et al. (2007) for multifractal analysis of a porous medium porosity and REV estimation. In this study, entropy dimension (DI^{i}) is tested to avoid unclear REV plateau in porosity curves. The entropy dimension (DI^{i}) of porosity is calculated by Eq. (14). Variation curves of entropy dimension (DI^{i}) for all observation cells (Fig. 2a) are presented in Fig. 4. The curves of entropy dimension (DI^{i}) of porosity and PCE saturation generally result in the increasing trend curves which makes REV estimates become very difficult and invalid. Entropy dimension (DI^{i}) was quickly increased with increasing of measured cuboid window size. Compared to the coefficient of variation (C_{V}^{i}) of porosity and PCE saturation, entropy dimension (DI^{i}) increased step by step without opposite fluctuation tendency in the variation curves as the length scale of measured cuboid window increased simultaneously. In general, REV plateau in region II (Fig. 1a) of porosity is not obvious for the entropy dimension (DI^{i}) curves of all observation cells from three experiments, which suggests REV scales is uneasy to identify for translucent silica using entropy dimension (DI^{i}) by light transmission technique.

3.1.3 The relative gradient error

The relative gradient error (ε_{g}^{i}) of porosity and PCE saturation is calculated by Eq. (17). The variation of ε_{g}^{i} at different measured cuboid window scales is shown in Fig. 4 for all observation cells in the 2D translucent silica. For all ε_{g}^{i} curves at observation cells from experiments, the REV plateaus in region II (Fig. 1a) are more clear than the variation curves based on the criteria of C_{V}^{i} and DI^{i}. Apparently, erratic variations of

the relative gradient error (ε_g^i) at small measured cuboid window scales are observed for

all ε_g^i curves as the characteristic of REV region I in Fig. 1a. When measured cuboid

window scale further increases for all observation cells, the variability and magnitude of

the relative gradient error (ε_g^i) decrease well and factor into average, which can be

identified as REV plateau in region II (Fig. 1a). The relative gradient error (ε_g^i) makes the

REV plateau quantification convenient for all observation cells. At the measured cuboid

window size above the REV plateau, ε_g^i curves result in large variability for observation

cells I-1~2. These findings suggest that that the relative gradient error (ε_g^i) can make the

REV plateau more obvious, which greatly contribute to convenient and applicable REV

quantification for translucent silica by light transmission technique. However, random

fluctuations exist in ε_g^i curves visually, which make the REV plateau uneasy to identify

accurately.

3.1.4 The new criterion (χ^i)

χ^i of porosity and PCE saturation changing with measured cuboid window size is

shown in Fig. 4. Like the region I (Fig. 1a), erratic and random fluctuations appear at

small measured cuboid window sizes and χ^i increases with the increase of the measured

cuboid window size. When measured scale increases, the values of χ^i for all observation

cells appear fast reduction and rapidly tend to steady, which exhibit the characteristic of

REV plateau as measured scale reaches region II. The χ^i for observation cells restores the

erratic variation state of increasing trend after measured cuboid window size exceeding the

REV plateau. As shown in the variation curves of χ^i for all observation cells, the beginning

of the REV flat plateaus can be identified easily, suggesting χ^i is more convenient and

337 reliable than other methods for REV estimation. All observation cells show similar variation

338 curves of χ^i that low value intervals are quite apparent, indicating that χ^i is very effective to

339 make the REV plateau obvious for translucent silica used in this study. Using the criterion

340 of χ^i, the REV plateau of region II is flat, which is easily identified, compared with other

341 criteria for observation cells (Figs. 4a and b).

342 3.2 REVs of material properties

343 Based on the REV plateau identifications using the coefficient of variation

344 (C_V^i),entropy dimension (DI^i), the relative gradient error (ε_g^i) and the proposed new

345 criterion χ^i in Figs. 4a and b, the new criterion χ^i appears to be the most appropriate criterion

346 for REV plateau identification. Even though the relative gradient error (ε_g^i) can also make

347 REV plateau obvious, but various random fluctuations weaken the method and reduce the

348 associated accuracy. Therefore, REVs of porosity, density, tortuosity and PCE plume are

349 estimated using the new criterion χ^i in the following study.

350 In fact, large number of discretized cells in the 2D translucent silica for three

351 experiments are quantified using the new criterion χ^i, which is convenient to examine the

352 regularities for REV sizes and related factors. Using the new criterion χ^i, the REV estimation

353 is conducted based on Eq. (18). Fig. 5a shows minimum REV sizes of porosity, density and

354 tortuosity quantified by χ^i for all cells of three experiments. Associated statistical analysis

355 for REVs is illustrated in Fig. 5b, where circular points represent frequency and triangular

356 points represent cumulative frequency. Frequency of REVs is dense in the middle and sparse

357 on both sides, so the distribution of REVs can be fitted by Gaussian equation:

$$F = \omega + \frac{1}{\sqrt{2\pi}\epsilon} e^{-\frac{(REV-v)^2}{2\epsilon^2}} \qquad (19)$$

359   where F is the frequency of REV; ω, ϵ and ν are fitted parameters of the model.

360   After regression analysis, the derived models for REV frequency are listed in Table 2.

361   The coefficients of determination (R^2) of models for REVs of porosity and density for three

362   experiments all exceed 0.85. R^2 for REV of tortuosity for three experiments exceeds 0.76.

363   Moreover, the computed cumulative frequency based on models fit cumulative frequency

364   from experimental results well in Fig. 5b.

365   The minimum REV size frequency of porosity appears a peak between 4.0 mm and 5.0

366   mm for Experiment-I. As minimum REV size of porosity increases, corresponding

367   frequency continuously decreases. Further, smooth convex shape of cumulative frequency

368   is observed for minimum REV size of porosity (Fig. 5b). Most minimum REV sizes of

369   translucent silica distributed in 0.0-7.0mm. For density of translucent silica sand, associated

370   REV frequency appears high values between 2.0~3.0 mm. For the REV sizes of tortuosity,

371   minimum REV sizes distribute in 0.0~6.0 mm. Compared with Experiment-I (F40/50 mesh

372   translucent silica sand), the frequency of REV for Experiment-II (F20/30 mesh translucent

373   silica sand with larger porosity) shows flat shape and has larger value of standard deviation,

374   especially for REV of porosity. Fig. 5b shows that translucent silica with larger porosity will

375   achieve border distribution of minimum REV sizes distribution compared to translucent

376   silica with relative lower porosity. Moreover, the frequency of REV of porosity and

377   permeability for Experiment-III (background material is F20/30 mesh translucent silica sand

378   with larger porosity, five lenses with lower porosity is packed in sandbox to create

379   heterogeneity) is similar to the frequency of REV for Experiment-II. However, the

380   frequency of τ-REV for Experiment-III is different from the frequency of τ -REV for

381   Experiment-II under homogeneous condition. The mean REV sizes of porosity, density and

382   tortuosity for Experiment-I are 4.35 mm, 2.89 mm and 3.65 mm, respectively. All mean

383   REV sizes of these variables for Experiment-II are larger than REVs of Experiments-I,

384   which corresponding mean REV sizes are 8.05 mm, 2.97 mm and 4.30 mm. These results

385   suggest translucent porous media with higher porosity lead to larger values of mean and

386   standard deviation for REV sizes.

387   3.3 REVs of S_o and A_{OW} for PCE plume

388   Based on the new criterion χ^i and light transmission technique, the real-time

389   distributions of S_o-REV and A_{OW}-REV for PCE plume can be obtained over the entire

390   experimental period. The minimum REV sizes of S_o and A_{OW} obtained using new criterion

391   χ^i are shown in Figs. 6a and b. When PCE migrates in sandbox, the REV of PCE plume is

392   changed over time (Fig. 6). The REVs of PCE plume for Experiment-I mostly are lower

393   than the REVs of PCE plume for Experiments-II and III. Moreover, when heterogeneous

394   porous media is packed in sandbox, the REV distribution of Experiment-III become more

395   heterogeneous compared with REV distribution of Experiments-II under homogeneous

396   condition. Based on REV distributions of PCE plume for three experiments, statistical

397   analysis is conducted to explore the regularity of REV distribution for PCE plume.

398   The mass center coordinate of PCE plume, GTP and plume area are shown in Fig. 7a.

399   The values of X_m, Z_m and GTP for Experiment-II and III are higher than the X_m, Z_m and

400   GTP of Experiment-I (lower porosity). Moreover, the plume area of Experiment-II is larger

401   than the plume of Experiment-I. When packed material is heterogeneous, the plume area of

402   PCE is increased further for Experiment-III. Besides, the mean and standard deviation of

REVs of PCE plume during 0~1523 min are derived by statistical analysis (Fig. 7a). Compared with REVs of PCE plume for Experiment-I, Experiment-II (F20/30 mesh translucent silica sand with higher porosity) has larger value of mean and standard deviation of REVs. The mean value of A_{OW}-REV for Experiment-III is much higher than A_{OW}-REV for Experiments-I and II.

The average value of REVs ($\overline{REV}$) and associated distance (d_m) from mass center to corresponding cells contained in PCE plume at t=1523 min are presented in Fig. 7b. Regression analysis is performed for average REVs of PCE plume and d_m, where fitted models and associated R^2 for Experiments-I-III are listed in Table 3. Simultaneously, the fitted equations between $\overline{REV}$ and d_I (the distance from injection point to cell contained in PCE plume) also are derived by regression analysis. From the results in Fig. 7a, $\overline{REV}$ of S_o and A_{ow} appear a peak and then decrease with increasing of d_m and d_I for Experiment-I. $\overline{REV}$ of S_o and A_{ow} for Experiment-I all firstly increase and then decrease with the increasing of d_m and d_I. However, $\overline{REV}$ of S_o presents apparent decreasing tendency as d_m and d_I increase for Experiment-II, and $\overline{REV}$ of A_{ow} just slightly increase first and then decrease for Experiment-II. In addition, the value of A_{OW}-REV mostly is higher than the value of S_o-REV for three experiments. Compared with the R^2 of the fitted relationship between average REVs of PCE plume and d_m, d_I for Experiments-I and II, the values of R^2 achieved by Experiment-III are much lower (Table 3).

Besides, the relationship between REVs and PCE saturation are fitted by regression analysis, where fitted equation and R^2 for three experiments are listed in Table 4 and Fig. 7b. With increasing of PCE saturation, REV of S_o appear decline trend for three experiments.

425   However, REV of A_{OW} increases when S_o increases for all three experiments (Fig. 7b). On

426   the other hand, REV of S_o for Experiment-II is higher than corresponding REV for

427   Experiment-I, while Experiments-I and II have similar values of A_{OW}-REV (Fig. 7b).

428   Moreover, REVs of S_o and A_{OW} for Experiment-III are higher than REVs of S_o and A_{OW} for

429   Experiments-I and II. These results suggest higher porosity will lead to high value of S_o-

430   REV and the relationship between REVs of PCE plume and dm, d$_I$. S_o-REV and A_{OW}-REV

431   are increased under heterogeneous condition.

432   **4. Conclusions**

433   In this study, a new criterion χ^i is proposed to identify the REVs of translucent porous

434   media and inner contaminant transformation based on previous criteria. The REV plateaus

435   of observation cells selected from three experiments of PCE transport are hard to judge

436   visually from the porosity and PCE saturation curves. From the REV identification effects

437   of different criteria, the REV flat plateau is difficult to identify by the coefficient of variation

438   (C_V^i) and entropy dimension (DI^i), indicting the coefficient of variation (C_V^i) and entropy

439   dimension (DI^i) are not suitable for REV estimation of translucent porous media. The

440   relative gradient error (ε_g^i) can make REV plateaus of all kinds of translucent silica

441   explicit in variation curves, but random fluctuations weaken REV plateau identification. In

442   comparison with these previous criteria, the beginning and ending of the REV flat plateaus

443   could be easily and directly identified in the curves based on the new criterion χ^i, suggesting

444   the new criterion χ^i is more convenient and effective for REV estimation. In this study, REVs

445   of porosity, density, tortuosity, and PCE plume are estimated using the new criterion χ^i.

446   Statistical results of minimum REV scales quantified by new criterion χ^i reveal

21

447 cumulative frequencies of porosity, density and tortuosity all have smooth convex shapes.

448 Models based on Gaussian equation are built for the distribution of REVs of porosity,

449 density and tortuosity, which porous media with larger porosity leads to larger values of

450 mean and standard deviation for REV sizes of media properties. For REVs of PCE plume,

451 result suggested larger porosity lead to larger value of mean and standard deviation.

452 Regression analysis is performed to study the regularity for distribution of REVs, where

453 fitted relationship between REVs and d_m, d_I are derived for PCE plume. $\overline{REV}$ of S_o and

454 A_{ow} firstly increase and then decrease with the increasing of d_m and d_I for Experiment-I

455 whose sandbox packed by translucent porous media with relatively lower porosity. However,

456 $\overline{REV}$ of S_o and A_{ow} directly decrease with the increment of d_m and d_I when porosity became

457 larger for Experiment-II. The values of R^2 of the fitted relationship between average REVs

458 of PCE plume and d_m, d_I for Experiment-III are much lower under heterogeneous condition.

459 Significantly, REV size of S_o presented decreasing trend as S_o increases, while increasing

460 tendency appeared for REV size of A_{ow}. Through regression analysis, the fitted equations

461 between REVs of PCE plume and PCE saturation are derived for three experiments.

462 Implications of these finding are essential for quantitative investigation of scale effect of

463 porous media and contaminant transformation. The fluid migration and transform in porous

464 media can be simulated accurately according to the REV estimation results using light

465 transmission technique and the appropriate criterion χ^i.

466 **Code and data availability**

467 The codes and data for this paper are available by contacting the corresponding author at

468   jfwu@nju.edu.cn.

Author contributions

470   Ming Wu: Conceptualization, Methodology, Writing;

471   Jianfeng Wu: Conceptualization, Methodology, Writing;

472   Jichun Wu: Conceptualization;

473   Bill X. Hu: Conceptualization, Writing.

Declaration of interests

475   The authors declare that they have no known competing financial interests or personal

476   relationships that could have appeared to influence the work reported in this paper.

Acknowledgments

References

486   Al-Raoush, R., and Papadopoulos, A.: Representative elementary volume analysis of porous

media using X-ray computed tomography, Power Technol., 200, 60-77, 2010.

Al-Raoush, R.: Change in Microstructure Parameters of Porous Media Over Representative Elementary Volume for Porosity, Part. Sci. Technol., 30, 1-16, 2012.

Bai, L., Wang, X., Chen, Q., Ye, Y., Zheng, H., Guo, J., Yin, Y., and Gao, C.: Explaining the Size Dependence in Platinum-Nanoparticle-Catalyzed Hydrogenation Reactions, Angew. Chem. Int. Ed., 55, 15656-15661, 2016.

Bob, M.M., Brooks, M.C., Mravik, S.C., and Wood, A.L.: A modified light transmission visualization method for DNAPL saturation measurements in 2-D models, Adv. Water Resour., 31, 727-742, 2008.

Borges, J.A.R., and Pires, L.F.: Representative elementary area (REA) in soil bulk density measurements through gamma ray computed tomography, Soil Till. Res., 123, 43-49, 2012.

Borges, JAR., Pires, L.F., Cássaro, F.A.M., Roque, W.L., Heck, R.J., Rosa, J.A., and Wolf, F.G.: X-ray microtomography analysis of representative elementary volume (REV) of soil morphological and geometrical properties, Soil Till. Res., 182, 112-122, 2018.

Bouvry, B., del Campo, L., Meneses, D.D.S., Rozenbaum, O., Echegut, R., Lechevalier, D., Gaubil, M., and Echegut, P.: Hybrid methodology for retrieving thermal radiative properties of semi-transparent ceramics, J. Phys. Chem. C, 120, 3267-3274, 2016.

Bradford, S.A., Vendlinski, R.A., and Abriola, L.M.: The entrapment and long-term dissolution of tetrachloroethylene in fractional wettability porous media, Water Resour. Res., 35(10), 295-2964, 1999.

Brown, G.O., and Hsieh, H.T.: Evaluation of laboratory dolomite core sample size using representative elementary volume concepts, Water Resour. Res., 36(5), 1199-1207, 2000.

Corbett, P.W.M., and Jensen, J.L.: Estimating the mean permeability: how many measurement do we need? First Break, 10(3), 89-94, 1992.

Costanza-Robinson, M.S., Estabrook, B.D., and Fouhey, D.F.: Representative elementary volume estimation for porosity, moisture saturation, and air-water interfacial areas in unsaturated porous media: Data quality implication, Water Resour. Res., 47, W07513, 2011.

Erning, K., Grandel, S., Dahmke, A., and Schäfe, D.: Simulation of DNAPL infiltration and spreading behavior in the saturated zone at varying flow velocities and alternating subsurface geometries, Environ. Earth Sci., 65, 1119-1131, 2012.

Esfandiar, A., Radha, B., Wang, F.C., Yang, Q., Hu, S., Garaj, S., Nair, R.R., Geim, A.K., and Gopinadhan, K.: Size effect in ion transport through angstrom-scale slits, Science, 358, 511-513, 2017.

Fernandes, J.S., Appoloni, C.R., and Fernandes, C.P.: Determination of the Representative Elementary Volume for the study of sandstones and siltstones by X-Ray microtomography, Mater. Res., 15(4), 662-670, 2012.

Ghilardi, P., Kai, A.K., and Menduni, G.: Self-similar heterogeneity in granular porous media at the representative elementary volume scale, Water Resour. Res., 29(4), 1205-1214, 1993.

Gilevska, T., Passeport, E., Shayan, M., Seger, E., Lutz, E.J., West, K.A., Morgan, S.A.,

531   Mack, E.E., and Lollar, B.S.: Determination of in situ biodegradation rates via a

532   novel high resolution isotopic approach in contaminated sediments, Water Res, 149,

533   632-639, 2019.

534   Hendrick, A.G., Erdmann, R.G., and Goodman, M.R.: Practical Considerations for

535   Selection of Representative Elementary Volumes for Fluid Permeability in Fibrous

536   Porous Media, Transp. Porous Med., 95, 389-405, 2012.

537   Kang, Q.J., Zhang, D.X., and Chen, S.Y.: Simulation of dissolution and precipitation in

538   porous media, J. Geophys. Res. 108, NO. B10, 2505, doi:10.1029/2003JB002504,

539   2003.

540   Kim, J., and Mohanty, B.P.: Influence of lateral subsurface flow and connectivity on soil

541   water storage in land surface modeling, J. Geophys. Res. Atmos., 121,704-721,

542   2016.

543   Lei, S., and Shi, Y.: Separate-phase model and its lattice Boltzmann algorithm for liquid-

544   vapor two-phase flows in porous media, Phys. Rev. E, 99, 053302, 2019.

545   Martínez, F.S.J., Caniego, F.J., García-Gutiérrez, C., and Espejo, R.: Representative

546   elementary area for multifractal analysis of soil porosity using entropy dimension,

547   Nonlin. Processes Geophys., 14, 503-511, 2007.

548   Müller, C., and Siegesmund, S.: Evaluation of the representative elementary volume (REV)

549   of a fractured geothermal sandstone reservoir, Environ. Earth Sci., 61, 1713-1724,

550   2010.

551   Niemet, M.R., and Selker, J.S.: A new method for quantification of liquid saturation in 2D

552   translucent porous media systems using light transmission, Adv. Water Resour., 24,

651-666, 2001.

Nordahl, K., and Ringrose, P.S.: Identifying the Representative Elementary Volume for permeability in heterolithic deposits using numerical rock models, Math Geosci., 40, 753-771, 2008.

O'Carroll, D.M., Bradford, S.A., and Abriola, L.M.: Infiltration of PCE in a system containing spatial wettability variations, J. Contam. Hydrol., 73, 39-63, 2004.

Pereira Nunes, J.P., Blunt, M.J., and Bijeljic, B.: Pore-scale simulation of carbonate dissolution in micro-CT images, J. Geophys. Res. Solid Earth, 121, 558-576, 2016.

Piccoli, I, Schjønning, P., Lamandé, M., Zanini, F., and Morari, F.: Coupling gas transport measurements and X-ray tomography scans for multiscale analysis in silty soils, Geoderma, 338, 576-584, 2019.

Razavi, M.R., Muhunthan, B., and Al Hattamleh, O.: Representative elementary volume analysis of sands using x-ray computed tomography, Geotech. Test J., 30(3), 212-219, 2007.

Rozenbaum, O., and du Roscoat, S.R.: Representative elementary volume assessment of three-dimensional x-ray microtomography images of heterogeneous materials:Application to limestones, Phys. Rev. E, 89, 053304, 2014.

Teruel, F.E., and Rizwan-uddin: Numerical computation of macroscopic turbulence quantities in representative elementary volumes of the porous medium, Int. J. Heat Mass Transfer., 53, 5190-5198, 2010.

Ukrainczyk, N., and Koenders, E.A.B.: Representative elementary volumes for 3D modeling of mass transport in cementitious materials, Modelling Simul. Mater. Sci.

575   Eng., 22, 035001, 2014.

576 Wang, L., Mi, J., and Guo, Z.: A modified lattice Bhatnagar–Gross–Krook model for

577   convection heat transfer in porous media, Int. J. Heat Mass Transfer., 94, 269-291,

578   2016.

579 Wang, S., Elsworth, D., and Liu, J.: A mechanistic model for permeability evolution in

580   fractured sorbing media, J. Geophys. Res, 117, B06205,

581   doi:10.1029/2011JB008855, 2012.

582 Wu, M., Wu, J.F., and Wu, J.C.: Simulation of DNAPL migration in heterogeneous

583   translucent porous media based on estimation of representative elementary volume,

584   J. Hydrol., 553, 276-288, 2017.

585 Wu, M., Wu, J.F., Wu, J.C., and Hu, B.X.: Effects of microarrangement of solid particles on

586   PCE migration and its remediation in porous media, Hydrol. Earth Syst. Sci., 22,

587   1001-1015, 2018.

588

589   **Table 1.** Experimental conditions

Experiment	I	II	III
Sandbox dimensions (cm)	20×15	60×45	60×45
Background translucent silica sand	F40/50	F20/30	F20/30
Medium condition	Homogeneity	Homogeneity	Heterogeneity
Median grain diameter (mm)	0.36	0.72	0.72
Permeability (m^2)	4.25×10^{-11}	1.35×10^{-10}	1.35×10^{-10}
V_{PCE} (ml)	9	32	40
Injection rate (ml/min)	0.5	0.5	0.5

590

591

592 **Table 2.** The <u>fitted parameters of the models</u>~~fitted equations~~ of frequency for REVs of

593 porosity, density and tortuosity

Experiment		I	II	III
θ-REV	ω	-2.11×10^{-4}	-1.45×10^{-3}	7.63×10^{-4}
	ϵ	1.73	3.45	3.18
	ν	4.35	7.90	6.50
	R^2	0.938	0.924	0.907
ρ-REV	ω	-6.51×10^{-4}	-2.51×10^{-4}	1.51×10^{-3}
	ϵ	1.08	1.66	2.40
	ν	2.89	2.97	3.70
	R^2	0.967	0.990	0.859
τ-REV	ω	-3.36×10^{-4}	-2.04×10^{-4}	1.29×10^{-3}
	ϵ	1.39	2.15	1.20
	ν	3.65	4.20	1.05
	R^2	0.769	0.875	0.919

594 [*]θ represents porosity, ρ represents density, τ represents tortuosity; ω, ϵ and ν are fitted parameters
595 of the model

596

597

598   **Table 3.** The fitted equations between average value of REV and d_I, d_m

Experiment		d_m	d_I
I	S_o-REV	$\overline{REV} = -1.67 \times 10^{-3}d_m^2 + 0.193d_m$ $+ 2.72$ (R^2=0.807)	$\overline{REV} = -1.97 \times 10^{-3}d_I^2 + 0.245d_I$ $+ 1.12$ (R^2=0.832)
	A_{OW}-REV	$\overline{REV} = -6.10 \times 10^{-4}d_m^2$ $+ 5.82 \times 10^{-2}d_m$ $+ 7.20$ (R^2=0.401)	$\overline{REV} = -1.47 \times 10^{-3}d_I^2 + 0.205d_I$ $+ 1.84$ (R^2=0.733)
II	S_o-REV	$\overline{REV} = -4.08 \times 10^{-5}d_m^2$ $+ 1.50 \times 10^{-2}d_m$ $+ 7.54$ (R^2=0.655)	$\overline{REV} = -3.94 \times 10^{-5}d_I^2$ $+ 7.80 \times 10^{-3}d_I$ $+ 8.50$ (R^2=0.327)
	A_{OW}-REV	$\overline{REV} = -1.92 \times 10^{-5}d_m^2$ $+ 4.47 \times 10^{-3}d_m$ $+ 9.46$ (R^2=0.616)	$\overline{REV} = -1.92 \times 10^{-5}d_I^2$ $+ 4.47 \times 10^{-3}d_I$ $+ 9.46$ (R^2=0.616)
III	S_o-REV	$\overline{REV} = -6.06 \times 10^{-6}d_m^2$ $+ 2.27 \times 10^{-3}d_m$ $+ 7.76$ (R^2=0.153)	$\overline{REV} = 1.69 \times 10^{-5}d_I^2$ $- 1.21 \times 10^{-2}d_I$ $+ 9.62$ (R^2=0.236)
	A_{OW}-REV	$\overline{REV} = -8.71 \times 10^{-6}d_m^2$ $+ 5.66 \times 10^{-3}d_m$ $+ 11.5$ (R^2=0.115)	$\overline{REV} = -1.50 \times 10^{-5}d_I^2$ $+ 7.88 \times 10^{-3}d_I$ $+ 11.4$ (R^2=0.150)

599   [*]$\overline{REV}$ is the average value of REV size, d_m is the distance from mass center of PCE plume

600   to the cell contained in PCE plume, d_I is the distance from injection point to the cell

601   contained in PCE plume

602

603

604 **Table 4.** The fitted relationship between REV and S_o

Experiment	S_o-REV	A_{OW}-REV
I	$REV = -2.13 \times \ln S_o + 0.876$ (R^2=0.466)	$REV = 2.27e^{2.70 \times S_o}$ (R^2=0.366)
II	$REV = -0.961 \times \ln S_o + 1.09$ (R^2=0.415)	$REV = 1.70e^{3.30 \times S_o}$ (R^2=0.500)
III	$REV = -1.40 \times \ln S_o + 3.96$ (R^2=0.538)	$REV = 2.05e^{3.22 \times S_o}$ (R^2=0.573)

605
606

Figure Captions

Figure 1. (a) Variable changes as measured scale (L) increment in conceptual curve

(Costanza-Robinson et al., 2011); (b) Scale effect and the cuboid image window

geometry; (c) System Device for acquisition of parameters (porosity and density,

etc.) of translucent material; (d) The infinitesimal selected from translucent porous

media packed in 2D sandbox.

Figure 2. (a) The system sandbox equipment of Experiment-I; (b) The system sandbox

equipment of Experiment-II; (c) The system sandbox equipment of Experiment-III

Figure 3. (a) The emergent light intensity, porosity, permeability and tortuosity of 2D

translucent silica sand for Experiments-I-III; (b) The PCE saturation of

Experiments-I-III during 0~1523 min and observation cells

Figure 4. (a) The change of porosity (θ), associated coefficient of variation (C_V^i), entropy

dimension (DI^i), the relative gradient error (ε_g^i), and new criterion-χ^i for observation

cells as cuboid window scale (L) increases; (b) The change of PCE saturation (S_o),

associated C_V^i, DI^i, ε_g^i, and χ^i for observation cells as cuboid window scale (L)

increases

Figure 5. (a) The distributions of minimum REV sizes of porosity, sand density and

tortuosity for Experiments-I-III; (b) The frequency of minimum REV sizes of
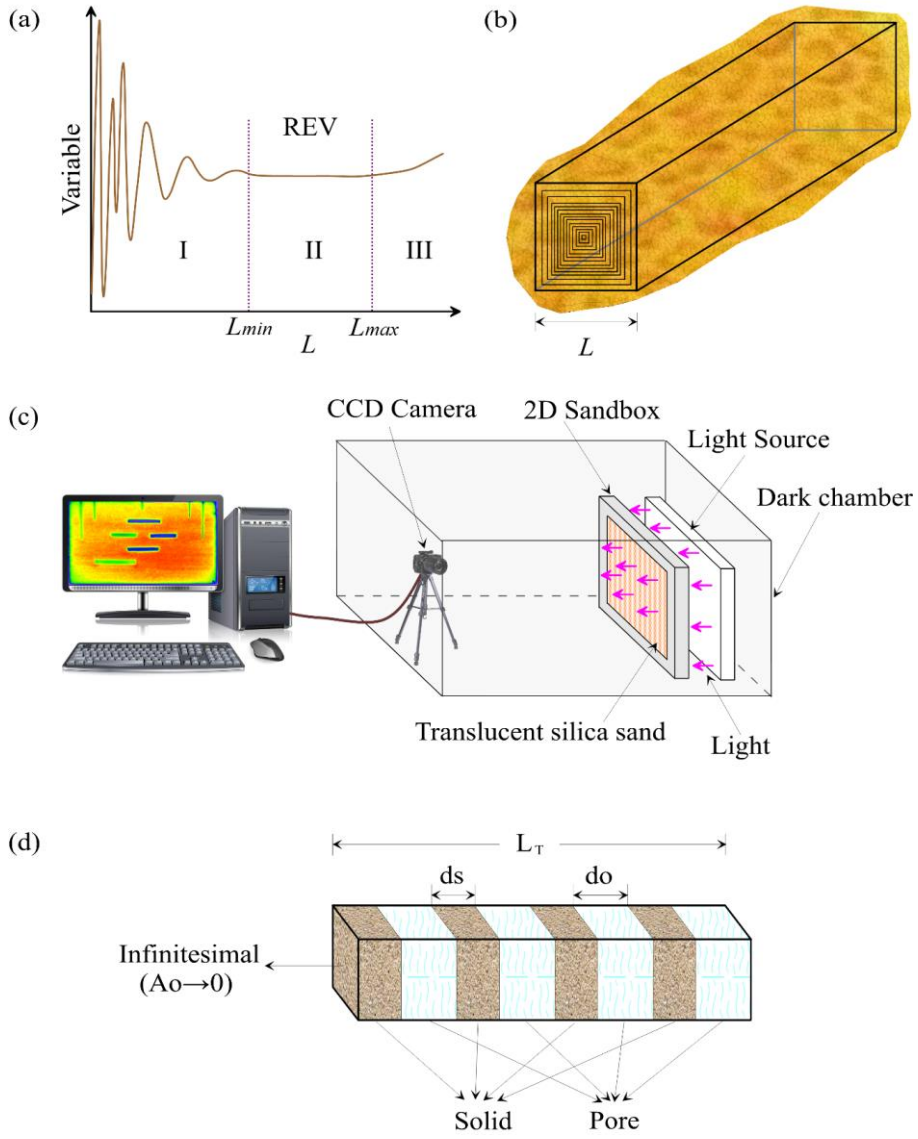
Experiments and fitted models

Figure 6. (a) The distributions of S_o-REV sizes during 0~1523 min for Experiments-I-III;

(b) The distributions of A_{OW}-REV sizes during 0~1523 min for Experiments-I-III

Figure 7. (a) The mass center coordinate of PCE plume, GTP, plume area and the mean,

standard deviation of S_o-REV and A_{OW}-REV during 0~1523 min; (b) The change of

630   average REV size as the distance d_I, d_m increases and fitted relationship between
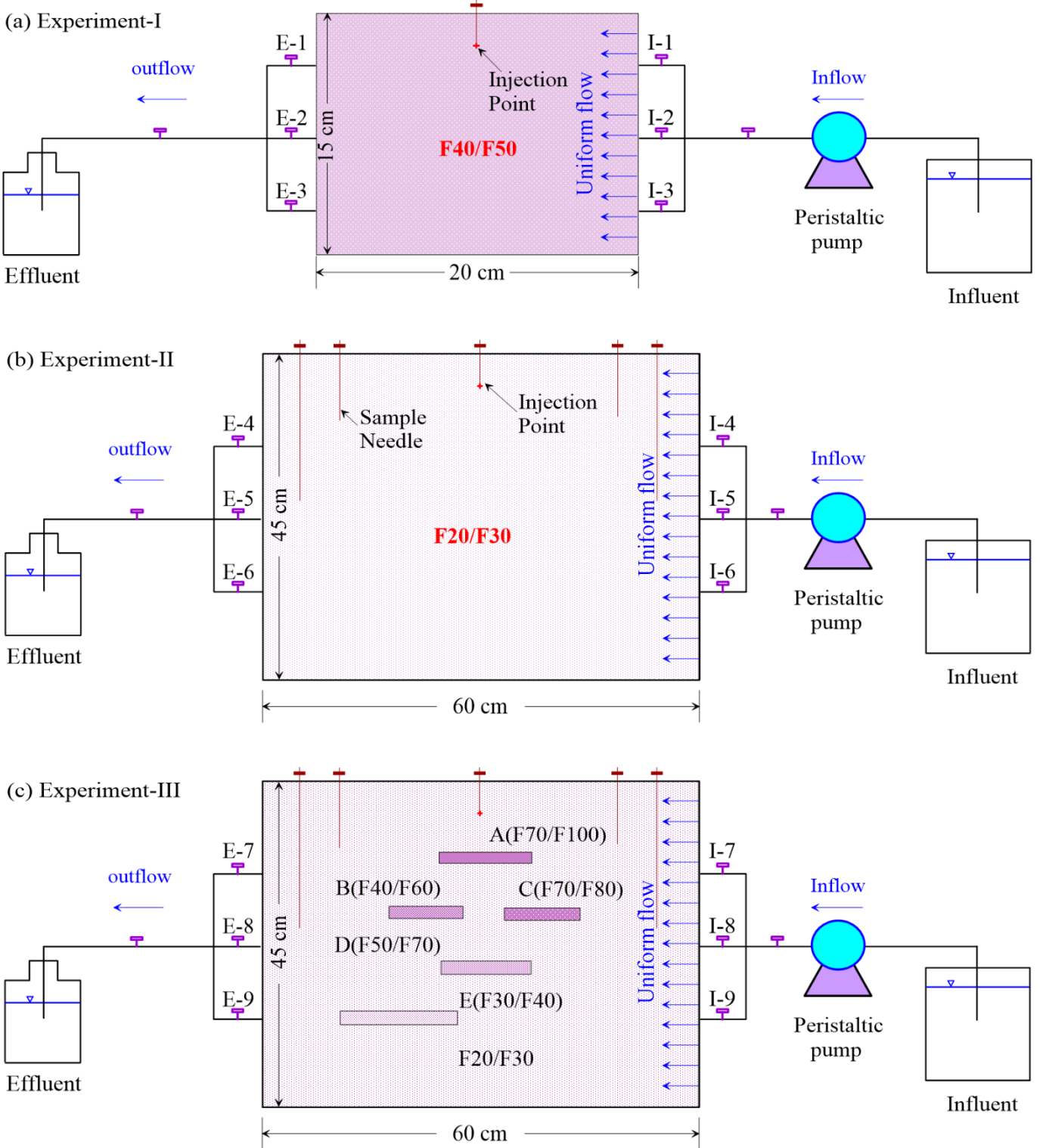
631   REV sizes and S_o for Experiments-I and II
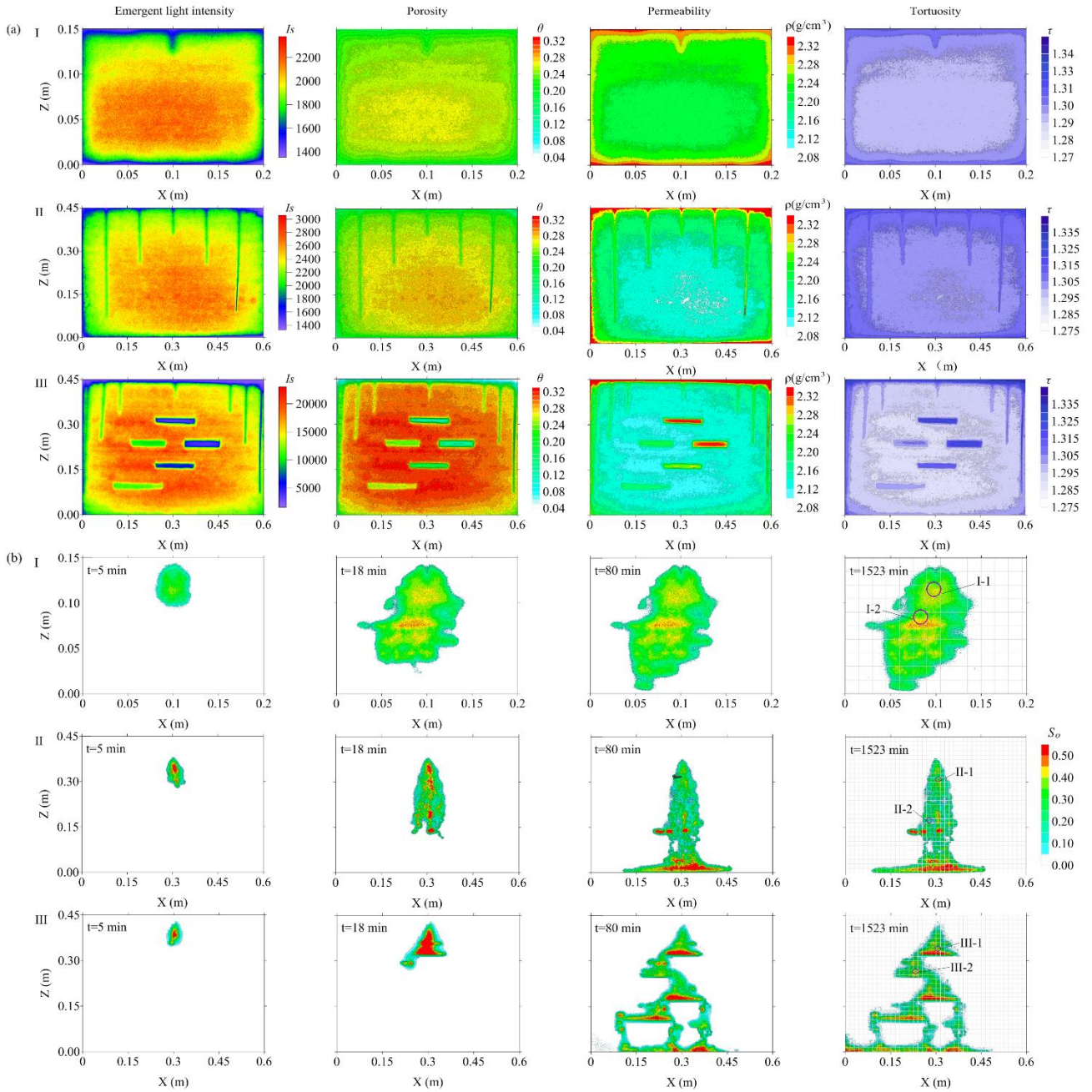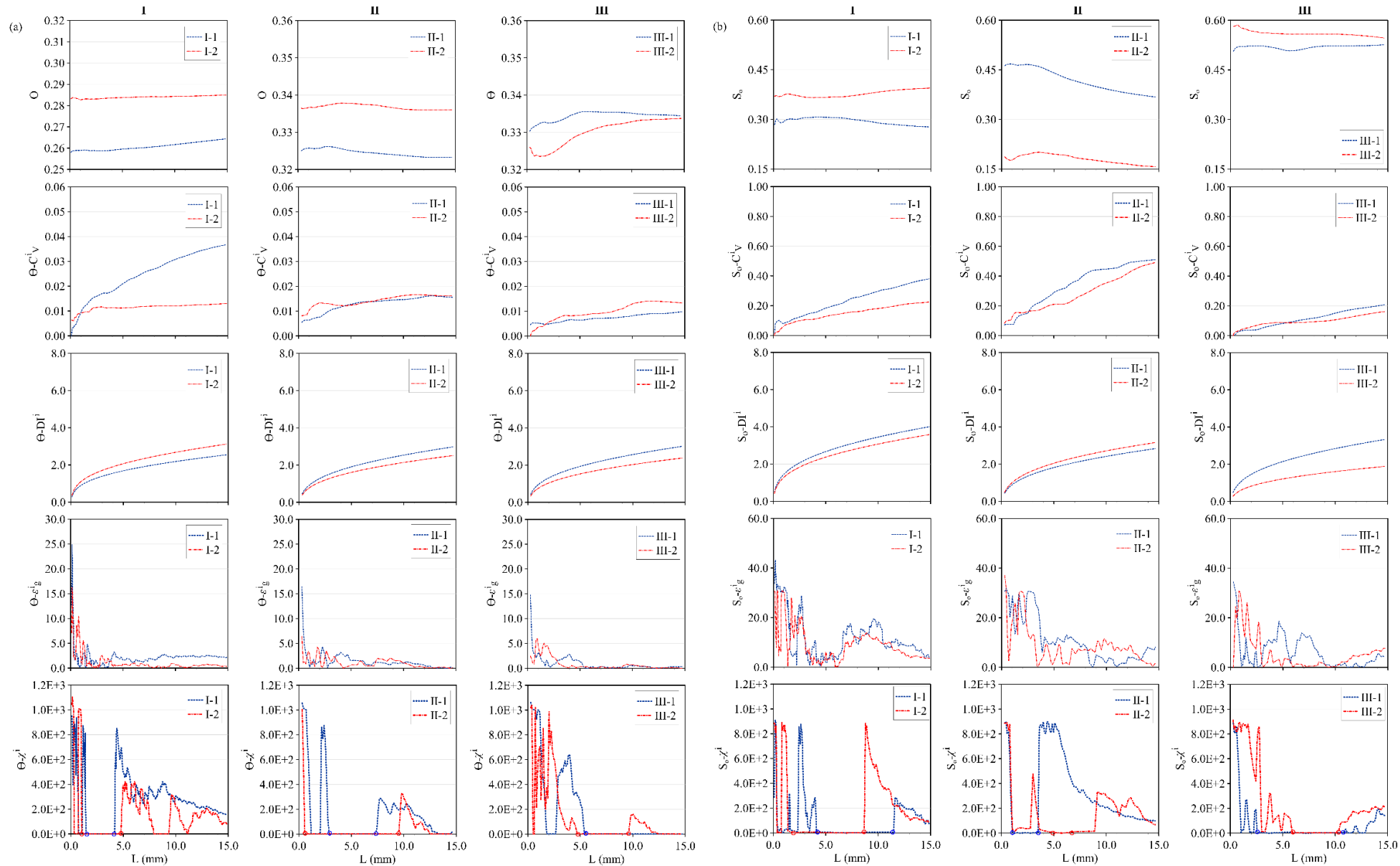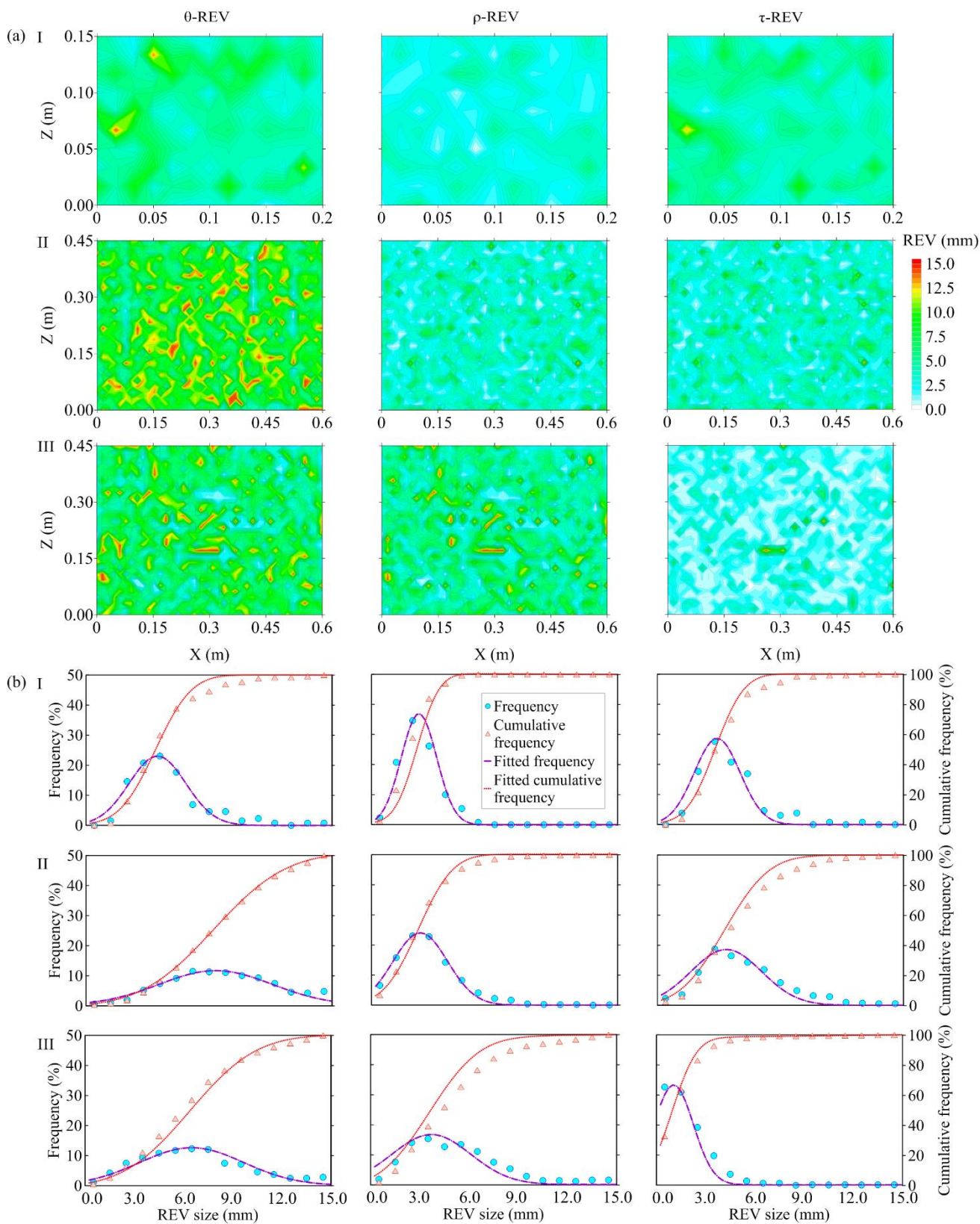
632   **Fig. 1**

633

634

635

Fig. 2

(a) Experiment-I

E-1

outflow

E-2   15 cm

Injection Point

F40/F50

E-3

Uniform flow

I-1

I-2

I-3

Inflow

Peristaltic pump

Effluent

20 cm

Influent

(b) Experiment-II

E-4

outflow

Sample Needle

Injection Point

E-5   45 cm

F20/F30

E-6

Uniform flow

I-4

I-5

I-6

Inflow

Peristaltic pump

Effluent

60 cm

Influent

(c) Experiment-III

E-7

outflow

A(F70/F100)

B(F40/F60)   C(F70/F80)

E-8   45 cm

D(F50/F70)

E-9

E(F30/F40)

F20/F30

Uniform flow

I-7

I-8

I-9

Inflow

Peristaltic pump

Effluent

60 cm

Influent

Fig. 3

Fig. 5

Fig. 6

40

654   **Fig. 7**

655

656